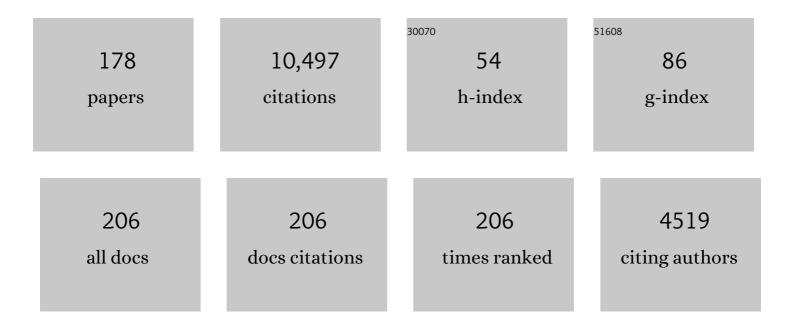
List of Publications by Year in descending order

Source: https://exaly.com/author-pdf/2492320/publications.pdf Version: 2024-02-01



#	Article	IF	CITATIONS
1	Vertical profiling of convective dust plumes in southern Morocco during SAMUM. Tellus, Series B: Chemical and Physical Meteorology, 2022, 61, 340.	1.6	68
2	Vertical profiling of Saharan dust with Raman lidars and airborne HSRL in southern Morocco during SAMUM. Tellus, Series B: Chemical and Physical Meteorology, 2022, 61, 144.	1.6	196
3	Desert dust aerosol air mass mapping in the western Sahara, using particle properties derived from space-based multi-angle imaging. Tellus, Series B: Chemical and Physical Meteorology, 2022, 61, 239.	1.6	57
4	Dust mobilization and transport in the northern Sahara during SAMUM 2006 – a meteorological overview. Tellus, Series B: Chemical and Physical Meteorology, 2022, 61, 12.	1.6	79
5	Regional Saharan dust modelling during the SAMUM 2006 campaign. Tellus, Series B: Chemical and Physical Meteorology, 2022, 61, 307.	1.6	48
6	Retrieval of aerosol optical thickness for desert conditions using MERIS observations during the SAMUM campaign. Tellus, Series B: Chemical and Physical Meteorology, 2022, 61, 229.	1.6	25
7	Spectral surface albedo over Morocco and its impact on radiative forcing of Saharan dust. Tellus, Series B: Chemical and Physical Meteorology, 2022, 61, 252.	1.6	68
8	Depolarization ratio profiling at several wavelengths in pure Saharan dust during SAMUM 2006. Tellus, Series B: Chemical and Physical Meteorology, 2022, 61, 165.	1.6	436
9	EARLINET observations of the 14–22-May long-range dust transport event during SAMUM 2006: validation of results from dust transport modelling. Tellus, Series B: Chemical and Physical Meteorology, 2022, 61, 325.	1.6	47
10	Measurements of desert dust optical characteristics at Porte au Sahara during SAMUM. Tellus, Series B: Chemical and Physical Meteorology, 2022, 61, 206.	1.6	21
11	Arctic haze over Central Europe. Tellus, Series B: Chemical and Physical Meteorology, 2022, 55, 796.	1.6	4
12	Profiling of Saharan dust and biomass-burning smoke with multiwavelength polarization Raman lidar at Cape Verde. Tellus, Series B: Chemical and Physical Meteorology, 2022, 63, 649.	1.6	128
13	Optical and microphysical properties of smoke over Cape Verde inferred from multiwavelength lidar measurements. Tellus, Series B: Chemical and Physical Meteorology, 2022, 63, 677.	1.6	90
14	Saharan Mineral Dust Experiments SAMUM–1 and SAMUM–2: what have we learned?. Tellus, Series B: Chemical and Physical Meteorology, 2022, 63, 403.	1.6	187
15	Regional modelling of Saharan dust and biomass-burning smoke: Part 1: Model description and evaluation. Tellus, Series B: Chemical and Physical Meteorology, 2022, 63, 781.	1.6	47
16	Optical properties of aerosol mixtures derived from sun-sky radiometry during SAMUM-2. Tellus, Series B: Chemical and Physical Meteorology, 2022, 63, 635.	1.6	58
17	Effect of internal mixture on black carbon radiative forcing. Tellus, Series B: Chemical and Physical Meteorology, 2022, 64, 10925.	1.6	60
18	LITES: rotational Raman spectra of air molecules measured by high-resolution-spectroscopy lidar. Optics Letters, 2021, 46, 5173.	3.3	3

#	Article	IF	CITATIONS
19	Measurement report: Balloon-borne in situ profiling of Saharan dust over Cyprus with the UCASS optical particle counter. Atmospheric Chemistry and Physics, 2021, 21, 6781-6797.	4.9	7
20	Lidar Innovations for Technologies and Environmental Sciences (LITES) – An Remote Sensing Infrastructure Facility: Setup and Measurements Examples. EPJ Web of Conferences, 2020, 237, 07017.	0.3	0
21	Application of Regularization Algorithm to HSRL-2 Observations During Oracles Campaign: Comparison of Retrieved and In Situ Particle Size Distributions and Single Scattering Albedo. EPJ Web of Conferences, 2020, 237, 02008.	0.3	0
22	3+2 + <i>X</i> : what is the most useful depolarization input for retrieving microphysical properties of non-spherical particles from lidar measurements using the spheroid model of Dubovik et al.Â(2006)?. Atmospheric Measurement Techniques, 2019, 12, 4421-4437.	3.1	16
23	Aerosol-type classification based on AERONET version 3 inversion products. Atmospheric Measurement Techniques, 2019, 12, 3789-3803.	3.1	52
24	Technical note: Absorption aerosol optical depth components from AERONET observations of mixed dust plumes. Atmospheric Measurement Techniques, 2019, 12, 607-618.	3.1	26
25	The unprecedented 2017–2018 stratospheric smoke event: decay phase and aerosol properties observed with the EARLINET. Atmospheric Chemistry and Physics, 2019, 19, 15183-15198.	4.9	83
26	Automated, unsupervised inversion of multiwavelength lidar data with TiARA: assessment of retrieval performance of microphysical parameters using simulated data. Applied Optics, 2019, 58, 4981.	1.8	17
27	A new method to retrieve the real part of the equivalent refractive index of atmospheric aerosols. Journal of Aerosol Science, 2018, 117, 54-62.	3.8	15
28	Synergy of lidar and passive remote sensor data for retrieving profiles of microphysical properties of non-spherical particles. EPJ Web of Conferences, 2018, 176, 08001.	0.3	0
29	Lidar sprectroscopy instrument (LISSI): An infrastructure facility for chemical aerosol profiling at the University of Hertfordshire. EPJ Web of Conferences, 2018, 176, 01008.	0.3	0
30	Aerosol absorption profiling from the synergy of lidar and sun-photometry: the ACTRIS-2 campaigns in Germany, Greece and Cyprus. EPJ Web of Conferences, 2018, 176, 08005.	0.3	5
31	On the spectral depolarisation and lidar ratio of mineral dust provided in the AERONET version 3 inversion product. Atmospheric Chemistry and Physics, 2018, 18, 12735-12746.	4.9	53
32	Improved identification of the solution space of aerosol microphysical properties derived from the inversion of profiles of lidar optical data, part 3: case studies. Applied Optics, 2018, 57, 2499.	1.8	5
33	Calibration of a high spectral resolution lidar using a Michelson interferometer, with data examples from ORACLES. Applied Optics, 2018, 57, 6061.	1.8	51
34	Variation of the vertical distribution of Nabro volcano aerosol layers in the stratosphere observed by LIDAR. Atmospheric Environment, 2017, 154, 1-8.	4.1	7
35	Depolarization ratios retrieved by AERONET sun–sky radiometer data and comparison to depolarization ratios measured with lidar. Atmospheric Chemistry and Physics, 2017, 17, 6271-6290.	4.9	30
36	HSRL-2 aerosol optical measurements and microphysical retrievals vs. airborne in situ measurements during DISCOVER-AQ 2013: an intercomparison study. Atmospheric Chemistry and Physics, 2017, 17, 7229-7243.	4.9	46

#	Article	IF	CITATIONS
37	Vertical Variation of Optical Properties of Mixed Asian Dust/Pollution Plumes According to Pathway of Airmass Transport Over East Asia. EPJ Web of Conferences, 2016, 119, 08001.	0.3	Ο
38	Microphysical particle properties derived from inversion algorithms developed in the framework of EARLINET. Atmospheric Measurement Techniques, 2016, 9, 5007-5035.	3.1	47
39	Arrange and Average Algorithm for Microphysical Retrievals with A "3β+3α―Lidar Configuration. EPJ Web of Conferences, 2016, 119, 23026.	0.3	0
40	Comparison of Aerosol Optical and Microphysical Retrievals from HSRL-2 and in-Situ Measurements During DISCOVER-AQ 2013 (California and Texas). EPJ Web of Conferences, 2016, 119, 23014.	0.3	0
41	Improved identification of the solution space of aerosol microphysical properties derived from the inversion of profiles of lidar optical data, part 1: theory. Applied Optics, 2016, 55, 9839.	2.1	14
42	Improved identification of the solution space of aerosol microphysical properties derived from the inversion of profiles of lidar optical data, part 2: simulations with synthetic optical data. Applied Optics, 2016, 55, 9850.	2.1	5
43	Tropospheric Vertical Profiles of Aerosol Optical, Microphysical and Concentration Properties in the Frame of the Hygra-CD Campaign (Athens, Greece 2014): A Case Study of Long-Range Transport of Mixed Aerosols. EPJ Web of Conferences, 2016, 119, 23016.	0.3	1
44	Gradient Correlation Method for the Stabilization of Inversion Results of Aerosol Microphysical Properties Retrieved from Profiles of Optical Data. EPJ Web of Conferences, 2016, 119, 23020.	0.3	0
45	Utilization of the depolarization ratio derived by AERONET Sun/sky radiometer data for type confirmation of a mixed aerosol plume over East Asia. International Journal of Remote Sensing, 2016, 37, 2180-2197.	2.9	7
46	Optical and microphysical characterization of aerosol layers over South Africa by means of multi-wavelength depolarization and Raman lidar measurements. Atmospheric Chemistry and Physics, 2016, 16, 8109-8123.	4.9	51
47	Vertical Resolved Dust Mass Concentration and Backscatter Coefficient Retrieval of Asian Dust Plume Using Quartz Raman Channel in Lidar Measurements. EPJ Web of Conferences, 2016, 119, 08004.	0.3	Ο
48	Perspectives of the Explicit Retrieval of the Complex Refractive Index of Aerosols from Optical Data Taken with Lidar. EPJ Web of Conferences, 2016, 119, 17016.	0.3	1
49	Influence of the vertical absorption profile of mixed Asian dust plumes on aerosol direct radiative forcing over East Asia. Atmospheric Environment, 2016, 138, 191-204.	4.1	17
50	Retrieval of aerosol parameters from multiwavelength lidar: investigation of the underlying inverse mathematical problem. Applied Optics, 2016, 55, 2188.	2.1	36
51	Vertically-resolved profiles of mass concentrations and particle backscatter coefficients of Asian dust plumes derived from lidar observations of silicon dioxide. Chemosphere, 2016, 143, 24-31.	8.2	8
52	Vertical variation of optical properties of mixed Asian dust/pollution plumes according to pathway of air mass transport over East Asia. Atmospheric Chemistry and Physics, 2015, 15, 6707-6720.	4.9	33
53	Aerosol optical and microphysical retrievals from a hybrid multiwavelength lidar data set – DISCOVER-AQ 2011. Atmospheric Measurement Techniques, 2014, 7, 3095-3112.	3.1	10
54	Retrieval of the single scattering albedo of Asian dust mixed with pollutants using lidar observations. Advances in Atmospheric Sciences, 2014, 31, 1417-1426.	4.3	10

#	Article	IF	CITATIONS
55	Airborne Multiwavelength High Spectral Resolution Lidar (HSRL-2) observations during TCAP 2012: vertical profiles of optical and microphysical properties of a smoke/urban haze plume over the northeastern coast of the US. Atmospheric Measurement Techniques, 2014, 7, 3487-3496.	3.1	79
56	Arrange and average algorithm for the retrieval of aerosol parameters from multiwavelength high-spectral-resolution lidar/Raman lidar data. Applied Optics, 2014, 53, 7252.	2.1	27
57	Influence of wind speed on optical properties of aerosols in the marine boundary layer measured by ship-borne DePolarization Lidar in the coastal area of Korea. Atmospheric Environment, 2014, 83, 282-290.	4.1	10
58	Dualâ€FOV Raman and Doppler lidar studies of aerosolâ€cloud interactions: Simultaneous profiling of aerosols, warmâ€cloud properties, and vertical wind. Journal of Geophysical Research D: Atmospheres, 2014, 119, 5512-5527.	3.3	25
59	The retrieval of the Asian dust depolarization ratio in Korea with the correction of the polarization-dependent transmission. Asia-Pacific Journal of Atmospheric Sciences, 2013, 49, 19-25.	2.3	15
60	Eruption of the Eyjafjallajökull Volcano in spring 2010: Multiwavelength Raman lidar measurements of sulphate particles in the lower troposphere. Journal of Geophysical Research D: Atmospheres, 2013, 118, 1804-1813.	3.3	38
61	Influence of biogenic pollen on optical properties of atmospheric aerosols observed by lidar over Gwangju, South Korea. Atmospheric Environment, 2013, 69, 139-147.	4.1	30
62	Vertical profiles of pure dust and mixed smoke–dust plumes inferred from inversion of multiwavelength Raman/polarization lidar data and comparison to AERONET retrievals and in situ observations. Applied Optics, 2013, 52, 3178.	1.8	61
63	Investigation of the diurnal pattern of the vertical distribution of pollen in the lower troposphere using LIDAR. Atmospheric Chemistry and Physics, 2013, 13, 7619-7629.	4.9	41
64	Studying Taklamakan aerosol properties with lidar (STAPL). Proceedings of SPIE, 2013, , .	0.8	2
65	Lidar profiling of aerosol optical and microphysical properties from space: overview, review, and outlook. , 2013, , .		1
66	Groundâ€based validation of CALIPSO observations of dust and smoke in the Cape Verde region. Journal of Geophysical Research D: Atmospheres, 2013, 118, 2889-2902.	3.3	70
67	Characterization of fresh and aged biomass burning events using multiwavelength Raman lidar and mass spectrometry. Journal of Geophysical Research D: Atmospheres, 2013, 118, 2956-2965.	3.3	89
68	Multi-wavelength Raman lidar, sun photometric and aircraft measurements in combination with inversion models for the estimation of the aerosol optical and physico-chemical properties over Athens, Greece. Atmospheric Measurement Techniques, 2012, 5, 1793-1808.	3.1	37
69	Lidar Measurements for Desert Dust Characterization: An Overview. Advances in Meteorology, 2012, 2012, 1-36.	1.6	88
70	Record heavy mineral dust outbreaks over Korea in 2010: Two cases observed with multiwavelength aerosol/depolarization/Ramanâ€quartz lidar. Geophysical Research Letters, 2012, 39, .	4.0	16
71	Atmospheric dust modeling from meso to global scales with the online NMMB/BSC-Dust model – Part 2: Experimental campaigns in Northern Africa. Atmospheric Chemistry and Physics, 2012, 12, 2933-2958.	4.9	87
72	Technical Note: One year of Raman-lidar measurements in Gual Pahari EUCAARI site close to New Delhi in India – Seasonal characteristics of the aerosol vertical structure. Atmospheric Chemistry and Physics, 2012, 12, 4513-4524.	4.9	63

#	Article	IF	CITATIONS
73	Estimation of radiative forcing by the dust and non-dust content in mixed East Asian pollution plumes on the basis of depolarization ratios measured with lidar. Atmospheric Environment, 2012, 61, 221-231.	4.1	26
74	Comparison of optical and microphysical properties of pure Saharan mineral dust observed with AERONET Sun photometer, Raman lidar, and in situ instruments during SAMUM 2006. Journal of Geophysical Research, 2012, 117, .	3.3	61
75	Aerosol profiling with lidar in the Amazon Basin during the wet and dry season. Journal of Geophysical Research, 2012, 117, .	3.3	95
76	Columnar aerosol optical and radiative properties according to season and air mass transport pattern over East Asia. Environmental Monitoring and Assessment, 2012, 184, 4763-4775.	2.7	6
77	Instantaneous Monitoring of Pollen Distribution in the Atmosphere by Surface-based Lidar. Korean Journal of Remote Sensing, 2012, 28, 1-9.	0.4	2
78	Retrieval of Pollen Optical Depth in the Local Atmosphere by Lidar Observations. Korean Journal of Remote Sensing, 2012, 28, 11-19.	0.4	1
79	Retrieval of Dust Backscatter Coefficient using Quartz Raman Channel in Lidar Measurements. Journal of Korean Society for Atmospheric Environment, 2012, 28, 86-93.	1.1	1
80	Optical and microphysical properties of fresh biomass burning aerosol retrieved by Raman lidar, and star-and sun-photometry. Geophysical Research Letters, 2011, 38, n/a-n/a.	4.0	117
81	Vertical profiles of microphysical particle properties derived from inversion with two-dimensional regularization of multiwavelength Raman lidar data: experiment. Applied Optics, 2011, 50, 2069.	2.1	22
82	Lidar measurements of Raman scattering at ultraviolet wavelength from mineral dust over East Asia. Optics Express, 2011, 19, 1569.	3.4	17
83	Vertically resolved light-absorption characteristics and the influence of relative humidity on particle properties: Multiwavelength Raman lidar observations of East Asian aerosol types over Korea. Journal of Geophysical Research, 2011, 116, .	3.3	32
84	The water vapour intercomparison effort in the framework of the Convective and Orographicallyâ€induced Precipitation Study: airborneâ€toâ€groundâ€based and airborneâ€toâ€airborne lidar systems. Quarterly Journal of the Royal Meteorological Society, 2011, 137, 325-348.	2.7	66
85	Atmospheric aerosol characterization combining multi-wavelength Raman lidar and MAX-DOAS measurements in Gwanjgu. , 2011, , .		1
86	Comparison of Raman Lidar Observations of Water Vapor with COSMO-DE Forecasts during COPS 2007. Weather and Forecasting, 2011, 26, 1056-1066.	1.4	6
87	EARLINET observations of the Eyjafjallaj $ ilde{A}f ilde{A}f ilde{A}$, $\hat{A}\P$ kull ash plume over Europe. , 2010, , .		9
88	Mineral dust observed with AERONET Sun photometer, Raman lidar, and in situ instruments during SAMUM 2006: Shapeâ€independent particle properties. Journal of Geophysical Research, 2010, 115, .	3.3	49
89	Mineral dust observed with AERONET Sun photometer, Raman lidar, and in situ instruments during SAMUM 2006: Shapeâ€dependent particle properties. Journal of Geophysical Research, 2010, 115, .	3.3	38
90	Estimation of the microphysical aerosol properties over Thessaloniki, Greece, during the SCOUTâ€O ₃ campaign with the synergy of Raman lidar and Sun photometer data. Journal of Geophysical Research, 2010, 115, .	3.3	15

#	Article	IF	CITATIONS
91	Saharan dust and heterogeneous ice formation: Eleven years of cloud observations at a central European EARLINET site. Journal of Geophysical Research, 2010, 115, .	3.3	102
92	Volcanic aerosol layers observed with multiwavelength Raman lidar over central Europe in 2008–2009. Journal of Geophysical Research, 2010, 115, .	3.3	73
93	Size matters: Influence of multiple scattering on CALIPSO lightâ€extinction profiling in desert dust. Geophysical Research Letters, 2010, 37, .	4.0	75
94	The 16 April 2010 major volcanic ash plume over central Europe: EARLINET lidar and AERONET photometer observations at Leipzig and Munich, Germany. Geophysical Research Letters, 2010, 37, .	4.0	202
95	Mineral quartz concentration measurements of mixed mineral dust/urban haze pollution plumes over Korea with multiwavelength aerosol Ramanâ€quartz lidar. Geophysical Research Letters, 2010, 37, .	4.0	20
96	Correction to "Volcanic aerosol layers observed with multiwavelength Raman lidar over central Europe in 2008–2009― Journal of Geophysical Research, 2010, 115, .	3.3	1
97	Depolarization Ratio Retrievals Using AERONET Sun Photometer Data. Journal of the Optical Society of Korea, 2010, 14, 178-184.	0.6	6
98	Possibilities of the multichannel lidar spectrometer technique for investigation of the atmospheric aerosols and pollutions. , 2010, , .		1
99	Investigation of Source Dependent Optical and Microphysical Characteristics of Aerosol Using Multi-wavelength Raman Lidar in Anmyun, Korea. Journal of Korean Society for Atmospheric Environment, 2010, 26, 554-566.	1.1	1
100	Portable Raman Lidar PollyXT for Automated Profiling of Aerosol Backscatter, Extinction, and Depolarization. Journal of Atmospheric and Oceanic Technology, 2009, 26, 2366-2378.	1.3	145
101	Water vapour intercomparison effort in the frame of the Convective and Orographicallyâ€induced Precipitation Study. , 2009, , .		0
102	EARLINET: the European Aerosol Research Lidar Network for the Aerosol Climatology on Continental Scale. , 2009, , .		1
103	Optical and microphysical properties of severe haze and smoke aerosol measured by integrated remote sensing techniques in Gwangju, Korea. Atmospheric Environment, 2009, 43, 879-888.	4.1	69
104	Measuring atmospheric composition change. Atmospheric Environment, 2009, 43, 5351-5414.	4.1	160
105	Spectral aerosol optical depth characterization of desert dust during SAMUM 2006. Tellus, Series B: Chemical and Physical Meteorology, 2009, 61, 216-228.	1.6	57
106	Systematic error of lidar profiles caused by a polarization-dependent receiver transmission: quantification and error correction scheme. Applied Optics, 2009, 48, 2742.	2.1	35
107	Dust and smoke transport from Africa to South America: Lidar profiling over Cape Verde and the Amazon rainforest. Geophysical Research Letters, 2009, 36, .	4.0	146
108	Vertically resolved separation of dust and smoke over Cape Verde using multiwavelength Raman and polarization lidars during Saharan Mineral Dust Experiment 2008. Journal of Geophysical Research, 2009, 114, .	3.3	292

#	Article	IF	CITATIONS
109	Evolution of the ice phase in tropical altocumulus: SAMUM lidar observations over Cape Verde. Journal of Geophysical Research, 2009, 114, .	3.3	128
110	Regional dust model performance during SAMUM 2006. Geophysical Research Letters, 2009, 36, .	4.0	41
111	Retrieval of Lidar Overlap Factor using Raman Lidar System. Journal of Korean Society for Atmospheric Environment, 2009, 25, 450-458.	1.1	3
112	Measurement of Optical Properties of Ice-crystal Cloud using LIDAR System and Retrieval of Its Radiative Forcing by Radiative Transfer Model. Journal of Korean Society for Atmospheric Environment, 2009, 25, 392-401.	1.1	0
113	Seasonal characteristics of lidar ratios measured with a Raman lidar at Gwangju, Korea in spring and autumn. Atmospheric Environment, 2008, 42, 2208-2224.	4.1	67
114	Retrieval of microphysical properties of aerosol particles from one-wavelength Raman lidar and multiwavelength Sun photometer observations. Atmospheric Environment, 2008, 42, 6398-6404.	4.1	20
115	Radiative and dynamic effects of absorbing aerosol particles over the Pearl River Delta, China. Atmospheric Environment, 2008, 42, 6405-6416.	4.1	60
116	Influence of Saharan dust on cloud glaciation in southern Morocco during the Saharan Mineral Dust Experiment. Journal of Geophysical Research, 2008, 113, .	3.3	156
117	Systematic lidar observations of Saharan dust over Europe in the frame of EARLINET (2000–2002). Journal of Geophysical Research, 2008, 113, .	3.3	295
118	Ten years of multiwavelength Raman lidar observations of freeâ€ŧropospheric aerosol layers over central Europe: Geometrical properties and annual cycle. Journal of Geophysical Research, 2008, 113, .	3.3	80
119	Theory of inversion with two-dimensional regularization: profiles of microphysical particle properties derived from multiwavelength lidar measurements. Applied Optics, 2008, 47, 4472.	2.1	36
120	Lidar Observations of the Vertical Aerosol Flux in the Planetary Boundary Layer. Journal of Atmospheric and Oceanic Technology, 2008, 25, 1296-1306.	1.3	48
121	Raman Lidar for Monitoring of Aerosol Pollution in the Free Troposphere. , 2008, , 155-166.		1
122	EARLINET correlative measurements for CALIPSO. , 2007, , .		9
123	Optimization of lidar data processing: a goal of the EARLINET-ASOS project. , 2007, , .		6
124	Multiwavelength Raman lidar observations of particle growth during long-range transport of forest-fire smoke in the free troposphere. Geophysical Research Letters, 2007, 34, .	4.0	71
125	Particle backscatter, extinction, and lidar ratio profiling with Raman lidar in south and north China. Applied Optics, 2007, 46, 6302.	2.1	59
126	Characterization of atmospheric aerosols with multiwavelength Raman lidar. Proceedings of SPIE, 2007, , .	0.8	1

#	Article	IF	CITATIONS
127	Aerosol indirect effects as a function of cloud top pressure. Journal of Geophysical Research, 2007, 112, .	3.3	16
128	Aerosolâ€ŧypeâ€dependent lidar ratios observed with Raman lidar. Journal of Geophysical Research, 2007, 112, .	3.3	442
129	Cirrus optical properties observed with lidar, radiosonde, and satellite over the tropical Indian Ocean during the aerosolâ€polluted northeast and clean maritime southwest monsoon. Journal of Geophysical Research, 2007, 112, .	3.3	64
130	Retrieval of Aerosol Microphysical Parameter by Inversion Algorithm using Multi-wavelength Raman Lidar Data. Journal of Korean Society for Atmospheric Environment, 2007, 23, 97-109.	1.1	3
131	Aerosol lofting from sea breeze during the Indian Ocean Experiment. Journal of Geophysical Research, 2006, 111, .	3.3	32
132	Strong particle light absorption over the Pearl River Delta (south China) and Beijing (north China) determined from combined Raman lidar and Sun photometer observations. Geophysical Research Letters, 2006, 33, .	4.0	46
133	Potential of lidar backscatter data to estimate solar aerosol radiative forcing. Applied Optics, 2006, 45, 770.	2.1	5
134	Particle extinction measured at ambient conditions with differential optical absorption spectroscopy 2 Closure study. Applied Optics, 2006, 45, 2295.	2.1	7
135	Retrieval of aerosol properties from combined multiwavelength lidar and sunphotometer measurements. Applied Optics, 2006, 45, 7429.	2.1	25
136	Particle extinction measured at ambient conditions with differential optical absorption spectroscopy 1 System setup and characterization. Applied Optics, 2005, 44, 1657.	2.1	10
137	Daytime operation of a pure rotational Raman lidar by use of a Fabry–Perot interferometer. Applied Optics, 2005, 44, 3593.	2.1	55
138	Information content of multiwavelength lidar data with respect to microphysical particle properties derived from eigenvalue analysis. Applied Optics, 2005, 44, 5292.	2.1	72
139	Microphysical aerosol parameters from multiwavelength lidar. Journal of the Optical Society of America A: Optics and Image Science, and Vision, 2005, 22, 518.	1.5	113
140	Ice formation in Saharan dust over central Europe observed with temperature/humidity/aerosol Raman lidar. Journal of Geophysical Research, 2005, 110, .	3.3	81
141	Raman lidar observations of aged Siberian and Canadian forest fire smoke in the free troposphere over Germany in 2003: Microphysical particle characterization. Journal of Geophysical Research, 2005, 110, .	3.3	207
142	High aerosol load over the Pearl River Delta, China, observed with Raman lidar and Sun photometer. Geophysical Research Letters, 2005, 32, .	4.0	72
143	Lidar and Atmospheric Aerosol Particles. , 2005, , 105-141.		82
144	Closure study on optical and microphysical properties of a mixed urban and Arctic haze air mass observed with Raman lidar and Sun photometer. Journal of Geophysical Research, 2004, 109, n/a-n/a.	3.3	37

#	Article	IF	CITATIONS
145	Characterization of Asian dust and Siberian smoke with multi-wavelength Raman lidar over Tokyo, Japan in spring 2003. Geophysical Research Letters, 2004, 31, .	4.0	182
146	Multiyear aerosol observations with dual-wavelength Raman lidar in the framework of EARLINET. Journal of Geophysical Research, 2004, 109, n/a-n/a.	3.3	136
147	Inversion of multiwavelength Raman lidar data for retrieval of bimodal aerosol size distribution. Applied Optics, 2004, 43, 1180.	2.1	140
148	Arctic haze over Central Europe. Tellus, Series B: Chemical and Physical Meteorology, 2003, 55, 796-807.	1.6	12
149	Optical properties of the Indo-Asian haze layer over the tropical Indian Ocean. Journal of Geophysical Research, 2003, 108, .	3.3	104
150	Saharan dust over a central European EARLINET-AERONET site: Combined observations with Raman lidar and Sun photometer. Journal of Geophysical Research, 2003, 108, .	3.3	98
151	Unexpectedly high aerosol load in the free troposphere over central Europe in spring/summer 2003. Geophysical Research Letters, 2003, 30, .	4.0	62
152	Indo-Asian pollution during INDOEX: Microphysical particle properties and single-scattering albedo inferred from multiwavelength lidar observations. Journal of Geophysical Research, 2003, 108, .	3.3	61
153	Long-range transport of Saharan dust to northern Europe: The 11-16 October 2001 outbreak observed with EARLINET. Journal of Geophysical Research, 2003, 108, n/a-n/a.	3.3	229
154	Vertical profiles of atmospheric particle parameters measured with a scanning 6-wavelength 11-channel aerosol lidar. , 2003, 5086, 139.		1
155	Inversion with regularization for the retrieval of tropospheric aerosol parameters from multiwavelength lidar sounding. Applied Optics, 2002, 41, 3685.	2.1	239
156	Relative-humidity profiling in the troposphere with a Raman lidar. Applied Optics, 2002, 41, 6451.	2.1	95
157	European pollution outbreaks during ACE 2: Optical particle properties inferred from multiwavelength lidar and star-Sun photometry. Journal of Geophysical Research, 2002, 107, AAC 8-1.	3.3	80
158	European pollution outbreaks during ACE 2: Microphysical particle properties and single-scattering albedo inferred from multiwavelength lidar observations. Journal of Geophysical Research, 2002, 107, AAC 3-1.	3.3	44
159	Dual-wavelength Raman lidar observations of the extinction-to-backscatter ratio of Saharan dust. Geophysical Research Letters, 2002, 29, 20-1-20-4.	4.0	162
160	Airborne observations of dry particle absorption and scattering properties over the northern Indian Ocean. Journal of Geophysical Research, 2002, 107, INX2 34-1.	3.3	12
161	An intercomparison of aerosol light extinction and 180° backscatter as derived using in situ instruments and Raman lidar during the INDOEX field campaign. Journal of Geophysical Research, 2002, 107, INX2 13-1.	3.3	31
162	Optical and microphysical characterization of biomass- burning and industrial-pollution aerosols from- multiwavelength lidar and aircraft measurements. Journal of Geophysical Research, 2002, 107, LAC 7-1-LAC 7-20.	3.3	169

#	Article	IF	CITATIONS
163	Tropospheric aerosol layers after a cold front passage in January 2000 as observed at several stations of the German Lidar Network. Atmospheric Research, 2002, 63, 39-58.	4.1	7
164	Comparison of the radiative impact of aerosols derived from vertically resolved (lidar) and vertically integrated (Sun photometer) measurements: Example of an Indian aerosol plume. Journal of Geophysical Research, 2001, 106, 22861-22870.	3.3	17
165	Comprehensive particle characterization from three-wavelength Raman-lidar observations: case study. Applied Optics, 2001, 40, 4863.	2.1	88
166	European pollution outbreaks during ACE 2: Lofted aerosol plumes observed with Raman lidar at the Portuguese coast. Journal of Geophysical Research, 2001, 106, 20725-20733.	3.3	76
167	Vertical profiling of optical and physical particle properties over the tropical Indian Ocean with six-wavelength lidar: 1. Seasonal cycle. Journal of Geophysical Research, 2001, 106, 28567-28575.	3.3	55
168	Vertical profiling of optical and physical particle properties over the tropical Indian Ocean with six-wavelength lidar: 2. Case studies. Journal of Geophysical Research, 2001, 106, 28577-28595.	3.3	51
169	One-year observations of particle lidar ratio over the tropical Indian Ocean with Raman lidar. Geophysical Research Letters, 2001, 28, 4559-4562.	4.0	65
170	Temperature profiling in the atmosphere using lidars. , 2001, 4397, 453.		1
171	<title>Aerosol characterization with advanced aerosol lidar for climate studies</title> . , 2000, 4341, 390.		0
172	Scanning 6-Wavelength 11-Channel Aerosol Lidar. Journal of Atmospheric and Oceanic Technology, 2000, 17, 1469-1482.	1.3	123
173	Microphysical particle parameters from extinction and backscatter lidar data by inversion with regularization: experiment. Applied Optics, 2000, 39, 1879.	2.1	64
174	Vertical profiling of the Indian aerosol plume with six-wavelength lidar during INDOEX: A first case study. Geophysical Research Letters, 2000, 27, 963-966.	4.0	90
175	Physical properties of the Indian aerosol plume derived from six-wavelength lidar Observations on 25 March 1999 of the Indian Ocean Experiment. Geophysical Research Letters, 2000, 27, 1403-1406.	4.0	40
176	Microphysical particle parameters from extinction and backscatter lidar data by inversion with regularization: theory. Applied Optics, 1999, 38, 2346.	2.1	309
177	Microphysical particle parameters from extinction and backscatter lidar data by inversion with regularization: simulation. Applied Optics, 1999, 38, 2358.	2.1	117
178	Retrieval of physical particle properties from lidar observations of extinction and backscatter at multiple wavelengths. Applied Optics, 1998, 37, 2260.	2.1	56